Measurement of fragmentation and functionalization pathways in the heterogeneous oxidation of oxidized organic aerosol

Jesse H. Kroll,[abc] Jared D. Smith,[d] Dung L. Che,[de] Sean H. Kessler,[b] Douglas R. Worsnop[c] and Kevin R. Wilson*[d]

Received 18th March 2009, Accepted 11th June 2009
First published as an Advance Article on the web 7th July 2009
DOI: 10.1039/b905289e

The competition between the addition of polar, oxygen-containing functional groups (functionalization) and the cleavage of C–C bonds (fragmentation) has a governing influence on the change in volatility of organic species upon atmospheric oxidation, and hence on the loading of tropospheric organic aerosol. However the relative importance of these two channels is generally poorly constrained for oxidized organics. Here we determine fragmentation–functionalization branching ratios for organics spanning a range of oxidation levels, using the heterogeneous oxidation of squalane ($C_{30}H_{62}$) as a model system. Squalane particles are exposed to high concentrations of OH in a flow reactor, and measurements of particle mass and elemental ratios enable the determination of absolute elemental composition (number of oxygen, carbon, and hydrogen atoms) of the oxidized particles. At low OH exposure, the oxygen content of the organics increases, indicating that functionalization dominates, whereas for more oxidized organics the amount of carbon in the particles decreases, indicating the increasing importance of fragmentation processes. Once the organics are moderately oxidized (O/C $\approx$ 0.4), fragmentation completely dominates, and the increase in O/C ratio upon further oxidation is due to the loss of carbon rather than the addition of oxygen. These results suggest that fragmentation reactions may be key steps in the formation and evolution of oxygenated organic aerosol (OOA).

Introduction

The earth's atmosphere contains a huge number of organic compounds, estimated to be in the tens to hundreds of thousands of individual species.[1] Many, if not most, of these species are directly involved in the formation and/or evolution of organic particulate matter, either as precursors to secondary organic aerosol (SOA) or as aerosol components (or possibly as both). A quantitative and predictive understanding of organic aerosol, necessary for assessing the role of anthropogenic activity on human health, air quality, and climate, thus requires a detailed description of the concentrations, properties, and chemical transformations of a large number of organics. The treatment of so many species presents substantial challenges for all areas of atmospheric chemistry: the laboratory study of photochemical reactions, the ambient measurement of atmospheric concentrations, and the development of accurate chemistry modules for use in chemical transport models.

Rather than attempt to describe all organic species explicitly, many laboratory and modeling studies treat organic aerosol (and SOA in particular) by lumping organics by vapor pressure.[2,3] Using this approach, SOA formation is described in terms of only a few surrogate compounds (two in the case of the "two-product model",[2] 5–10 in the case of the "volatility basis set"[3]), substantially simplifying a highly chemically complex system. The assumption in such a treatment is that the amounts and properties of these lumped species can be informed by experimental studies of SOA production. However, laboratory chamber studies generally access initial oxidation reactions only, typically those that a hydrocarbon undergoes in its first several ($\leq$12) hours in the atmosphere. By contrast, the atmospheric lifetime of a submicron particle is of the order of 5–12 days,[4] during which time it may be subject to many more generations of oxidation than are usually accessed in the laboratory. The products of this additional oxidative processing are likely to have properties (volatility, solubility, *etc.*) substantially different than those generated in chamber studies and included in SOA modules; this disconnect may contribute to the discrepancies in SOA loading between models and ambient measurements.[5–7]

Recently Donahue *et al.*[3] suggested that multigenerational oxidation can be included within lumped SOA modules by use of a "transformation matrix", which describes how vapor pressures of (lumped) organic species change upon further

[a] *Department of Civil and Environmental Engineering, Massachusetts Institute of Technology, Cambridge, MA 02139, USA*
[b] *Department of Chemical Engineering, Massachusetts Institute of Technology, Cambridge, MA 02139, USA*
[c] *Center for Aerosol and Cloud Chemistry, Aerodyne Research Inc., Billerica, MA 01821, USA*
[d] *Chemical Sciences Division, Lawrence Berkeley National Laboratory, Berkeley, CA 94720, USA. E-mail: KRWilson@lbl.gov; Tel: +1 510-495-2474*
[e] *Department of Chemistry, University of California, Berkeley, CA 94720, USA*

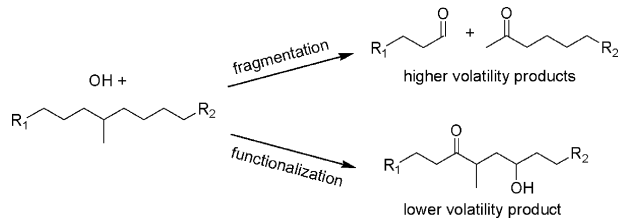

Fig. 1 Example of fragmentation and functionalization pathways in the atmospheric oxidation of an organic compound. In the oxidation of particulate organics, fragmentation leads to a loss of carbon from the particle (assuming at least one of the fragments is volatile), whereas functionalization leads to an increase in particulate oxygen.

oxidation. However, at present such a matrix can be informed only by chemical intuition rather than by experimental results, due to the lack of laboratory data constraining the effects of atmospheric processing on organic volatility. This is a source of significant uncertainty in models that include the effects of multigenerational oxidation on aerosol loading.[8–10]

An improved treatment of oxidative processing of organics within chemical transport models requires a quantitative description of how the volatilities of organic species are affected by atmospheric oxidation reactions. In the gas phase, two main processes (shown in Fig. 1) affect the volatilities of organics: the addition of polar functional groups, which lowers vapor pressure, and the fragmentation of the carbon skeleton *via* C–C bond scission, which increases vapor pressure. (In the condensed phase, additional bimolecular processes, such as accretion/oligomerization reactions,[11–13] can also affect volatility.) A key determinant of the changes to the volatility of organic species (and to the loading of organic aerosol) upon atmospheric oxidation is thus the competition between these functionalization and fragmentation reactions. This is reasonably well-studied in the case of the oxidation of alkanes, alkenes, and other reduced organics.[14–17] However, in the case of oxidized species, which make up the majority of organic particulate matter[18] and which serve as reactants in multigenerational oxidative processing, the competition between fragmentation and functionalization has received far less study. This arises in part from experimental constraints, since highly oxidized atmospheric organics in general are poorly characterized chemically, are present within complex mixtures, and are not commercially available. The lack of understanding of the chemical evolution of oxidized organics in the atmosphere severely limits our ability to accurately model the effects of photochemical processing reactions on atmospheric organic aerosol.

In this work we present the first measurements of the relative importance of fragmentation and functionalization reactions of organic species spanning a wide range in oxidation. The chemical system studied is the heterogeneous oxidation of particle-phase squalane (2,6,10,15,19,23-hexamethyltetracosane, $C_{30}H_{62}$) by gas-phase OH radicals. The heterogeneous oxidation of particulate organics makes for an ideal model system in that both functionalization and fragmentation reactions can be probed using current analytical techniques: increases in the oxygen content of the aerosol (as measured by high-resolution mass spectrometry) indicate functionalization reactions, whereas decreases in particle mass indicate fragmentation reactions. Squalane particles are exposed to a very wide range of OH exposures, with upper levels corresponding to several weeks of atmospheric oxidation. This is more oxidation than particulate organics would experience in their atmospheric lifetimes; however, the goal of this high level of exposure to oxidants is not the simulation of the atmospheric oxidation of reduced (hydrocarbon-containing) aerosol but rather the generation followed by further oxidation of highly oxidized organics. This therefore allows for the investigation of fragmentation–functionalization branching ratios for oxidized chemical species, such as those in SOA.

This work builds directly on our earlier study of the uptake coefficient and chemical mechanism of the OH + squalane reaction.[19] In that work it was shown that after substantial oxidation, reactions leading to particle volatilization become important, a result broadly consistent with results from other heterogeneous oxidation studies.[20,21] The present work is aimed at quantifying the importance of such volatilization reactions as a function of the O/C ratio of the organics, as well as assessing the possible role of functionalization and fragmentation reactions in the formation of oxidized organic aerosol (OOA) in the atmosphere.

Experimental

The experiments and experimental setup used here are the same as described by Smith *et al.*,[19] so only a brief description is provided here. A simple schematic of the reactor for the heterogeneous oxidation of organic particles is shown in Fig. 2. The flow reactor consists of a type-219 quartz tube (130 cm long, 2.5 cm id), with a residence time of 37 s (total flow 1 l min^{-1}). The carrier flow is N_2–O_2 (95 : 5), with a water bubbler to keep the flow at 30% relative humidity. Polydispersed submicron squalane particles are generated upstream of the reactor using a 125 °C nucleation oven. The particle size distribution is log-normal, with a geometric standard deviation of ~1.3, and a mean surface-weighted

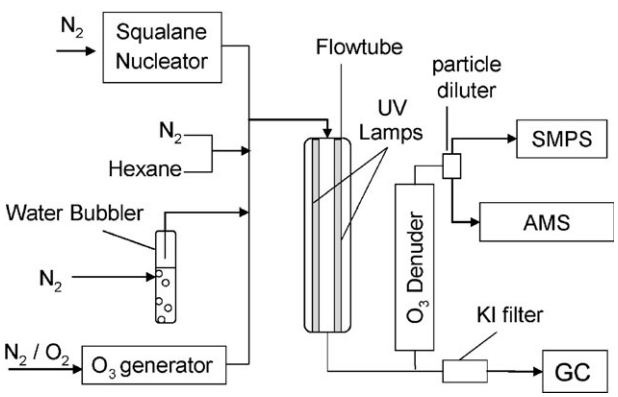

Fig. 2 Schematic of the flow reactor used in the present experiments. Squalane particles are generated in a nucleation oven and are exposed to high levels of OH generated from the 254 nm photolysis of ozone in the presence of water vapor. OH concentration is monitored by measuring the loss of a hexane tracer using GC-FID. Reacted particles are characterized using a scanning mobility particle sizer (SMPS) and a high-resolution time-of-flight aerosol mass spectrometer (AMS), for the measurement of particle mass and elemental composition.

diameter of ~160 nm. Ozone (10–200 ppm) is generated upstream by irradiation of an N_2–O_2 mixture with Hg pen-ray lamp or a corona discharge ozone generator (OzoneLab Instruments), and is measured with a commercial ozone monitor (2B Technologies). Two mercury lamps placed alongside the flow reactor provide 254 nm light (the quartz blocks shorter UV wavelengths), efficiently photolyzing ozone. The resulting $O(^1D)$ reacts with water vapor to generate OH radicals, initiating heterogeneous reaction. Because of the high water vapor concentrations, $O(^1D)$ concentrations are sufficiently low that virtually all oxidation of organics is by the OH radical, with a negligible ($\leq$1%) contribution by $O(^1D)$ radicals.[19]

OH exposure in the flow tube is monitored using a tracer technique. Small amounts (75–120 ppb) of hexane are introduced into the tube, and the measurement of the amount of hexane lost, using a preconcentrator-GC-FID system (SRI Instruments), enables the determination of the OH concentration.[19] At the highest OH exposures used here, nearly all of the hexane would be removed if it were allowed to react for the full 37 seconds. Under these conditions the hexane is injected near the end of the flow tube with a re-entrant tube and so has an OH exposure that is only a fraction of that of the entire flow tube. The fractional OH exposure is then converted to total OH exposure by a multiplicative factor. This factor is determined by injecting hexane first into the beginning of the reactor and then separately through the re-entrant tube at relatively low OH exposures. Under these conditions OH exposures are low enough that some hexane remains in either case. As we have previously reported,[19] at these low OH exposures the particle-phase O/C ratios are linearly proportional to the measured OH exposures. Thus the correction factor is determined by ensuring that the dependence of measured aerosol O/C ratio (described below) on OH exposure is the same for either configuration (with and without the re-entrant tube).

OH concentrations in the flow tube are controlled by changes to ozone, and range from 1.2×10^{10} to 7.4×10^{11} cm^{-3}, several (4–6) orders of magnitude higher than under typical ambient conditions. If all kinetic processes are first-order with respect to OH, such differences will not affect the product distribution, since all chemistry will scale linearly with OH concentration and exposure time. However, processes that are zeroth-order (such as photolysis) or second-order (such as radical–radical reactions) with respect to OH could potentially affect product formation in a nonlinear fashion, making extrapolation down to atmospheric conditions difficult. In a recent study we found little evidence that such processes play a major role in the chemistry, as products are essentially unchanged when squalane is exposed to much lower concentrations ($1–7 \times 10^8$ cm^{-3}) of OH, over longer timescales (1.5–3 hours).[22] At the same time, it was found that the OH uptake coefficient was somewhat higher at the lower OH concentrations, suggesting some role of secondary chemistry.[22] The implications of this chemistry for the extrapolation of flow tube data down to tropospheric conditions will be investigated in future work.

Two instruments are used to characterize the particles exiting the flow reactor, a scanning mobility particle sizer (SMPS, TSI) and a high-resolution time-of-flight aerosol mass spectrometer (HR-ToF-AMS, Aerodyne Research[23,24]). Just prior to measurement by the instruments, the particles are diluted by a factor of ~3–10, in order to keep measured mass concentrations in the range 10–100 μg m^{-3}. Measurement occurs within 1–3 seconds after dilution, which is too short for any appreciable repartitioning of semivolatile species.[25]

The AMS is used to measure elemental ratios of the particulate organics. The instrument used in these experiments has been modified to allow for vacuum ultraviolet photoionization of the aerosol components,[19,26] but for the experiments described here only electron impact ionization (EI) is used. Because all ions in the mass spectrum can be unambiguously identified, high-resolution EI mass spectrometry allows for the determination of relative abundances of different elements in a sample, namely the oxygen-to-carbon (O/C) and hydrogen-to-carbon (H/C) molar ratios.[27,28] The intensities of all organic ions below m/z 100 (including CO_2^+ and CO^+) are measured directly, though water-derived ions (H_2O^+, OH^+, and O^+) may also have inorganic sources and so their contributions to organic signal were estimated using the multiplicative relation between CO_2^+ and H_2O^+ (0.225) suggested by Aiken *et al.*[28] All AMS signals could be adequately fit by using ions composed only of C, O, and H atoms; as expected, no other elements were detected in the particles.

As demonstrated by Aiken *et al.*,[27,28] the elemental ratios determined from EI need to be corrected for biases arising from ion fragmentation within the mass spectrometer. Here we apply the empirical multiplicative factor of 1.33 to all O/C measurements.[28] No correction is applied for the H/C ratio, as the recommended multiplicative factor (1.1) was found to lead to an overestimate in the H/C ratio for squalane (and other alkanes). However, since the subsequent data analysis (described in the following section) is mass-based, results are insensitive to this value. These factors are somewhat uncertain (errors of ~30%[27]), and may even change with as the aerosol becomes increasingly oxidized. It is difficult to estimate how such changes might quantitatively affect our results, but they are unlikely to alter the overall conclusions of this work. We note that the multiple oxidation reactions form a complex mixture of a large number of products, for which the correction factors determined by Aiken *et al.*[27,28] are likely to be the most valid, due to the averaging of multiple correction factors for individual molecules.

Particle mass is obtained by combining SMPS and AMS data. Since squalane is a liquid at room temperature, the particles generated are spherical, enabling a straightforward calculation of total volume concentrations from SMPS measurements of size distributions (16–400 nm). Volume concentrations are divided by total particle number to yield average volume per particle. The ratio of vacuum aerodynamic diameters (as measured by the AMS[23]) and mobility diameters (as measured by the SMPS) yields particle density,[29] which when multiplied by SMPS volume gives particle mass on a per-particle basis. This mass measurement is independent of the collection efficiency of the AMS, which might change as a function of oxidation.

For the experiments reported here, the mass and elemental composition of the oxidized squalane particles are measured

over a wide range of OH exposures. After several minutes of data collection (corresponding to 1–2 SMPS scans) at a single OH exposure, the ozone concentration is changed in order to attain a different OH level in the flow reactor. The system is then allowed to equilibrate for a few minutes before AMS, SMPS, and GC-FID measurements are made at the new OH exposure. For some experiments the AMS and SMPS are placed downstream of a thermodenuder (TSI, residence time = 1.6 s), in order to measure particle volatility.

Results

Presented in Table 1 and Fig. 3 are results from the mass measurements and elemental analysis of the organic particles as a function of extent of oxidation. Oxidation is expressed in terms of "squalane oxidation lifetimes", which is the number of reactions with OH that an average squalane molecule has undergone; this is equal to the number of reactive OH collisions with the particle divided by the number of molecules in the particle.[19] This quantity is not strictly the same as "generation number", as at any given time the reaction products will be a statistical mixture of products from different (1st, 2nd, 3rd...) generations of reaction.[19] The number of squalane lifetimes is given by:

$$\text{lifetimes} = \frac{\Delta t}{\tau_{sq}} = k[\text{OH}]\Delta t \qquad (1)$$

in which Δt is exposure time (37 s), τ_{sq} the timescale of the oxidative loss of squalane, k is the measured second-order rate constant, and [OH] is the measured concentration of gas-phase OH. Lifetimes can instead be calculated from particle size, particle density, uptake coefficient, and molecular weight of the reactive organics,[30] but since we directly measure the oxidative loss of the squalane,[19] we can determine the value of k directly from our experiments and such a calculation is unnecessary. After substantial reaction (several lifetimes), the squalane molecules will have all reacted away, so "squalane lifetimes" may no longer accurately describe the average number of reactions the organics have undergone. However this is difficult to correct for, as it requires detailed characterization of reaction products (with uptake coefficients, molecular weights, *etc.*), which is not currently possible. This uncertainty in the degree to which the organics have reacted with OH does not affect the data or conclusions of this work, though determination of a simple, size-independent metric for the "extent of oxidation" in a complex multi-component aerosol would be extremely useful.

Table 1 Changes to aerosol properties upon heterogeneous oxidation

Lifetimes	Volume (norm.)	Density/ g cm^{-3}	Mass (norm.)	O/C ratio	H/C ratio
0.0	1.00	0.90	1.00	0.00	2.11
0.6	1.02	0.94	1.06	0.03	2.02
1.1	1.02	0.94	1.06	0.05	1.96
1.4	1.00	0.95	1.06	0.06	1.92
1.8	1.00	0.97	1.08	0.08	1.88
3.0	0.93	1.04	1.07	0.11	1.81
3.8	0.89	1.07	1.06	0.14	1.76
4.6	0.86	1.10	1.05	0.17	1.73
6.8	0.78	1.13	0.97	0.23	1.68
8.5	0.74	1.17	0.96	0.26	1.65
9.7	0.71	1.19	0.93	0.28	1.64
10.8	0.68	1.24	0.94	0.29	1.63
11.8	0.66	1.25	0.92	0.31	1.62
12.7	0.64	1.25	0.89	0.32	1.61
14.0	0.62	1.25	0.87	0.33	1.61
15.6	0.59	1.29	0.85	0.35	1.60
16.7	0.58	1.30	0.84	0.36	1.59
25.6	0.49	1.32	0.72	0.42	1.58
35.8	0.46	1.37	0.70	0.45	1.57

Measurements of particle volume (normalized to the initial volume per particle of the unreacted squalane), density, and mass (also normalized) are shown in Fig. 3a. At the initial onset of oxidation, the particle volume increases slightly and then stays roughly constant with oxidation. Upon further oxidation it then begins decreasing substantially, by over a factor of 2 at the highest oxidation levels (see Table 1). Density increases essentially monotonically with oxidation, from 0.90 g cm^{-3} for the unreacted organic to 1.37 g cm^{-3} for the most oxidized organics. This substantial increase in density as the organics become increasingly oxidized is consistent with measurements of the density of SOA spanning a range of oxidation levels.[31,32] The particle mass, determined by multiplying particle volume by density (and normalizing), increases slightly at first, a result of the increase in oxygen content of the organics (though the formation of SOA from the oxidation of squalane vapor may also make a minor contribution). Particle mass then decreases with further oxidation, indicating volatilization of the organics *via* fragmentation reactions. At the highest amount of oxidation studied, the mass per particle is ~30% lower than for unreacted squalane; however, as noted earlier[19] the total volatilization of organics is substantially greater than that, since the addition of oxygen increases the mass of the particles. These results are in agreement with those obtained for the heterogeneous oxidation of bis(2-ethylhexyl) sebacate,[20] though those results covered a somewhat smaller range in OH exposure and thus less volatilization was observed.

Shown in Fig. 3b are elemental ratios (O/C and H/C) of the particles, as determined by the HR-ToF-AMS. The oxygen-to-carbon ratio increases continually as a function of the extent of oxidation, as expected. The hydrogen-to-carbon ratio initially decreases, indicating an increase in the degree of unsaturation of the organic molecules, presumably from the formation of new C=O double bonds in aldehyde and ketone functional groups. After further oxidation this decrease is less dramatic, suggesting the increasing importance of C–O single bonds, most likely in carboxylic acid groups.

The degree to which functionalization reactions (which add oxygen) and fragmentation reactions (which remove carbon) occur can be quantified by absolute molar elemental abundances (the number of atoms of a given element in the particle phase). These can be calculated from particle mass, which is equal to the sum of the masses of the elements in the particle (in this case, carbon, oxygen, and hydrogen), and the measured elemental (H/C and O/C) ratios. Elemental abundance of carbon (nC) is computed as:

$$n\text{C} = \frac{M}{12 + 16\,(\text{O/C}) + (\text{H/C})} \qquad (2)$$

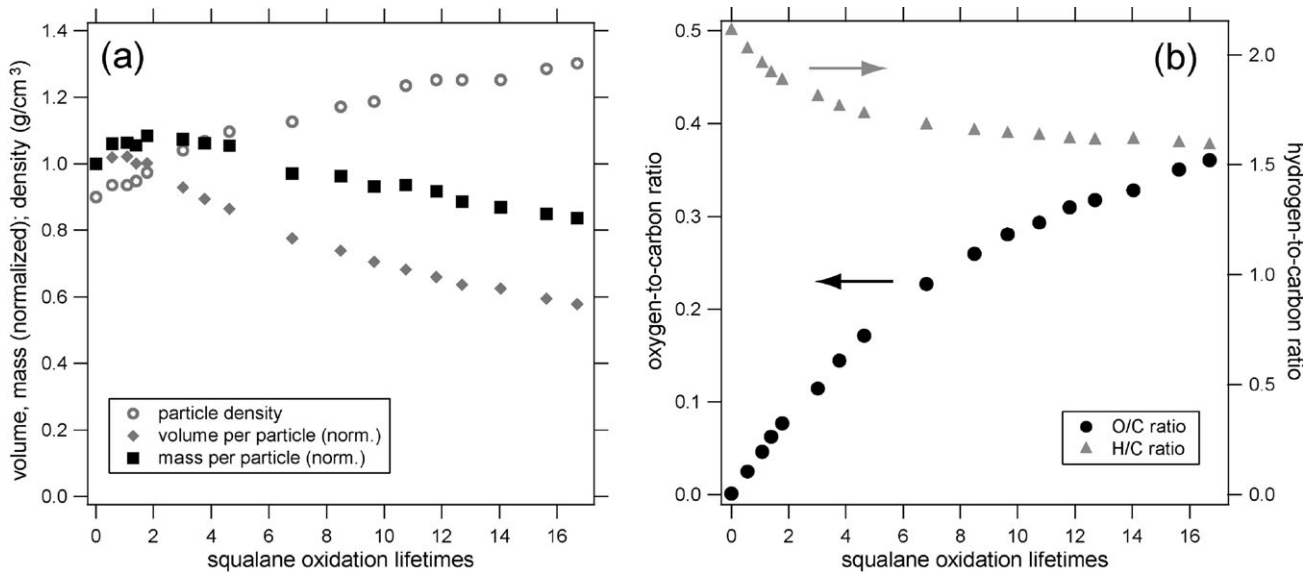

Fig. 3 Results from AMS and SMPS measurements of the heterogeneously oxidized particles. Panel (a): particle volume, density, and mass (volume and mass are normalized to the per-particle values for unreacted squalane). Panel (b): elemental (O/C and H/C) ratios of organic aerosol. Extent of oxidation (*x*-axis) is expressed in terms of "squalane oxidation lifetimes", which is the number of reactions with OH that an average squalane molecule has undergone (see text). Not shown: values at the two highest extents of oxidation, at 25.6 and 35.8 lifetimes (see Table 1 for values).

in which M is particle mass and O/C and H/C are molar elemental ratios. Elemental abundances of oxygen and hydrogen (nO and nH) can then be computed from nC, O/C, and H/C. Elemental abundances (normalized to the initial amount of particulate carbon) are given in Table 2 and Fig. 4a. The absolute carbon content increases slightly ($\sim$4%) when oxidation is initiated, which might suggest a minor contribution from SOA formed by the oxidation of gas-phase squalane. After this initial increase, further oxidation decreases the carbon content, indicating the onset of volatilization reactions; this decrease becomes quite dramatic after several lifetimes. The oxygen content increases essentially linearly with oxidation at first, which is consistent with our previous analysis.[19] However after a few lifetimes this increase in oxygen begins to slow, and stops entirely at high OH exposure ($>$10 lifetimes), at which point the absolute oxygen content of the aerosol does not change with further oxidation. This indicates that the increase in the O/C ratio shown in Fig. 3b is governed not by the addition of oxygen, but instead by the loss of carbon.

From these changes in elemental composition upon heterogeneous oxidation, the branching ratios for fragmentation and functionalization reactions can be calculated. Assuming that fragmentation reactions are those leading to a decrease in carbon content (dC), and functionalization reactions are those leading to an increase in oxygen content (dO), the branching ratio for fragmentation is given by:

$$\mathrm{BR_{frag}} = \frac{\mathrm{dC}}{\mathrm{dC} + \mathrm{dO}} = \left(1 + \frac{\mathrm{dO}}{\mathrm{dC}}\right)^{-1} = \left(1 + \frac{\mathrm{dO}/\mathrm{d}\tau}{\mathrm{dC}/\mathrm{d}\tau}\right)^{-1} \quad (3)$$

where τ is the number of lifetimes (though this calculation is independent of the choice of oxidation metric). Because the individual measurements are too coarse to permit a numerical treatment, this expression is evaluated by fitting the data in Fig. 4a to simple functions and differentiating. The functions used are arbitrary ones that fit the data well: $A_1 + A_2/(\tau^2 + A_3)$ in the case of carbon content and $A_4(1 - \mathrm{e}^{-\tau/A_5})$ in the case of oxygen content (A_n values are fitted parameters). This treatment assumes that changes to oxygen and carbon content result from heterogeneous reactions only. Any gas-to-particle conversion processes (SOA formation or reactive uptake) would tend to increase the abundance of both elements in the particles, which would have little effect on eqn (3) unless such processes dominated the chemistry. Such a scenario is

Table 2 Absolute elemental composition of heterogeneously oxidized particles and inferred fragmentation branching ratios

Lifetimes	Carbon content[a]	Oxygen content[a]	Hydrogen content[a]	Branching ratio (fragmentation)[b]
0.0	1.00	0.00	2.11	0.00
0.6	1.04	0.03	2.10	0.12
1.1	1.02	0.05	2.00	0.22
1.4	1.00	0.06	1.92	0.28
1.8	1.01	0.08	1.91	0.35
3.0	0.97	0.11	1.75	0.53
3.8	0.93	0.13	1.65	0.61
4.6	0.90	0.16	1.57	0.68
6.8	0.79	0.18	1.33	0.79
8.5	0.76	0.20	1.26	0.84
9.7	0.73	0.20	1.19	0.86
10.8	0.72	0.21	1.18	0.88
11.8	0.70	0.22	1.13	0.89
12.7	0.67	0.21	1.08	0.91
14.0	0.65	0.21	1.05	0.92
15.6	0.63	0.22	1.00	0.93
16.7	0.61	0.22	0.97	0.94
25.6	0.50	0.21	0.79	0.98
35.8	0.48	0.22	0.75	1.00

[a] Absolute molar elemental abundance in the particle, normalized to the amount of carbon per unreacted squalane particle. [b] See text for details of calculation.

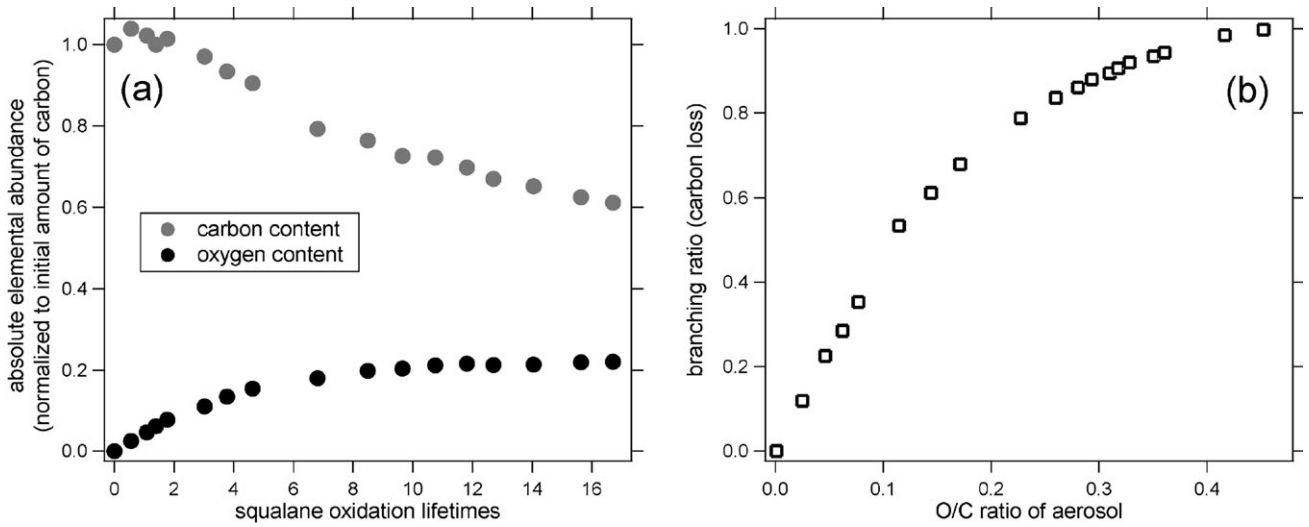

Fig. 4 Evolving particle chemistry, as calculated from the measurements of particle mass and elemental ratios. Panel (a): absolute molar abundances of carbon and oxygen in the particles (normalized to the amount of carbon per unreacted squalane particle). As in Fig. 3, the two points corresponding to the most oxidized organics are not shown (see Table 2 for values). With initial oxidation of the squalane, carbon content stays roughly constant (the slight increase may be from SOA formation) whereas oxygen content increases, indicating the importance of functionalization reactions. Further oxidation leads to the loss of carbon from the particles, indicating that fragmentation reactions are occurring. The increase in oxygen content then slows and stops completely, and the increase in O/C ratio (Fig. 3b) is driven entirely by carbon loss. Panel (b): calculated branching ratio for the loss of carbon (fragmentation) as a function of O/C ratio of the particulate organics. When the aerosol is moderately oxidized (O/C $\approx$ 0.4) fragmentation reactions completely dominate. It should be noted that these branching ratios may be strongly influenced by the details of the carbon skeleton of squalane; as discussed in the "Reaction mechanism" section, unbranched compounds may undergo substantially less fragmentation, particularly at lower O/C ratios.

highly unlikely given the large observed decrease in absolute carbon content of the particles (Fig. 4a).

Computed branching ratios are shown in Fig. 4b as a function of O/C ratio of the organic aerosol. For the least oxidized aerosol (unreacted squalane), functionalization dominates, with little contribution from fragmentation reactions. Fragmentation becomes increasingly important for more oxidized organics, and by the time the organics are moderately oxidized (O/C $\approx$ 0.4), fragmentation reactions completely dominate.

Reaction mechanism

The branching ratios between functionalization and fragmentation, shown in Fig. 4b, are determined on an elemental basis and so are not strictly the same as the corresponding branching ratios between molecular products (Fig. 1). For example, multiple atoms may be involved in a given reaction, with several carbon atoms lost to the gas phase *via* fragmentation, or multiple oxygen atoms added in a single functionalization reaction. In addition, fragmentation reactions might not lead to volatilization if both fragments are low in vapor pressure; these reactions would not be classified correctly using the present approach, which is based upon changes to particle mass. Nonetheless, such an atom-based description is useful for inclusion of multistep oxidation reactions (aging) within those models that express organic aerosol in terms of the number of carbon and/or oxygen atoms in the constituent organics.[8,33]

Describing reactions in terms of changes to the bulk elemental composition of organics provides no molecular information, such as the degree to which individual organic molecules fragment when particle mass decreases. Shown in Fig. 5 are two general chemical pathways by which volatilization can occur, with decreases in particulate carbon but no change in particulate oxygen. In pathway 1, both fragmentation products from the cleavage of the carbon skeleton are volatile and escape to the gas phase, leading to complete volatilization of the reacted molecule (1a). If this reaction occurs in parallel with a functionalization reaction (1b), there will be a loss of particulate carbon but no net change in particulate oxygen. (This pathway includes a functionalization reaction, but since it involves no change in particulate oxygen, it is considered a fragmentation reaction using our definition above.) In pathway 2, only one molecular fragment is volatile (as is the case for small organics, CO, or CO_2), and escapes into the gas phase, leading to a loss of particulate carbon. If the amount of oxygen added to the lower-volatility fragment (which remains in the particle) equals the amount lost to the gas phase, the net change in particulate oxygen will be zero.

These two possibilities do not differ substantially in changes to bulk elemental composition, but can be distinguished by changes in the volatility of the particulate organics. In the first pathway (complete volatilization), the organics remaining in the particle continue to decrease in volatility upon oxidation, as their carbon skeleton remains intact while polar functional groups are added. In the second (loss of small fragments), the decrease in volatility from the addition of oxygenated functional groups is offset by the loss of carbon, so that the overall change in volatility will be minor. Shown in Fig. 6 are the results from thermodenuder (TD) scans, expressed as mass fraction remaining *vs.* TD temperature, taken at two very

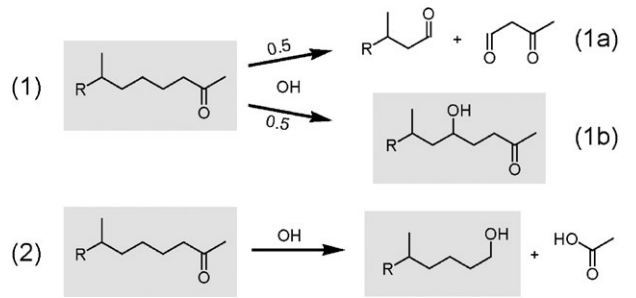

Fig. 5 General oxidative pathways that lead to the loss of particulate carbon but no change in particulate oxygen. Low-volatility (particle-phase) organics are shaded while volatile (gas-phase) organics are not. Pathway 1: formation of two volatile fragments (1a), leading to the complete volatilization of the molecule. If this is accompanied by an oxygen-addition reaction (1b), total particulate oxygen will stay constant. Pathway 2: loss of a single volatile species (CO, CO_2, or small organic) upon fragmentation. A key difference between the two channels is the volatilities of the particulate products.

different levels of OH exposure. The organics have undergone substantial oxidation between the two levels (5.1 and 10.1 lifetimes), so any changes in volatility should be obvious. The curves are almost identical, indicating that the additional oxidation has little effect on the volatility of the particulate organics. This suggests that fragmentation occurs *via* the loss of small volatile fragments from the organics in the particle (Fig. 5, pathway 2). Such a result is qualitatively consistent with the observation that the gas-phase products of heterogeneous oxidation reactions are, on average, relatively small (C1–C5).[34,35]

As discussed in a number of recent studies of the heterogeneous oxidation of organic species,[19–21,34–39] the volatilization (fragmentation) of condensed-phase organics likely arises from the dissociation of alkoxy radical intermediates.[14] The present results suggest that this dissociation channel dominates in the atmospheric oxidation of relatively oxidized organics. This is consistent with experimental evidence that oxygen-containing functional groups (carbonyls and alcohols) greatly increase the rates of alkoxy fragmentation reactions.[14] It is also consistent with other studies of heterogeneous oxidation that find evidence of volatilization when oxidation is highest.[20,21]

It should be noted that the fate of alkoxy radicals, and thus the fragmentation–functionalization branching ratio, is controlled not only by the presence of oxygen-containing functional groups, but also by structural details of the carbon skeleton.[14,17]. While the O/C ratios of the reacted organics were varied in this work, the carbon skeletons were not. Thus the branching ratios measured in this work (Fig. 4b) may be most applicable to organics that have similar structural features to squalane. In particular, squalane is highly branched, with six tertiary carbons that are expected to have a strong influence on the oxidation chemistry. Their hydrogens are highly susceptible to attack by OH (relative to primary and secondary hydrogens),[40] and so tertiary peroxy radicals will be formed in relatively high yields. In the subsequent $RO_2 + RO_2$ reaction, the Russell mechanism[41] is suppressed (due to the lack of α-hydrogens), so tertiary alkoxy radicals will be the dominant products. These radicals cannot react with O_2

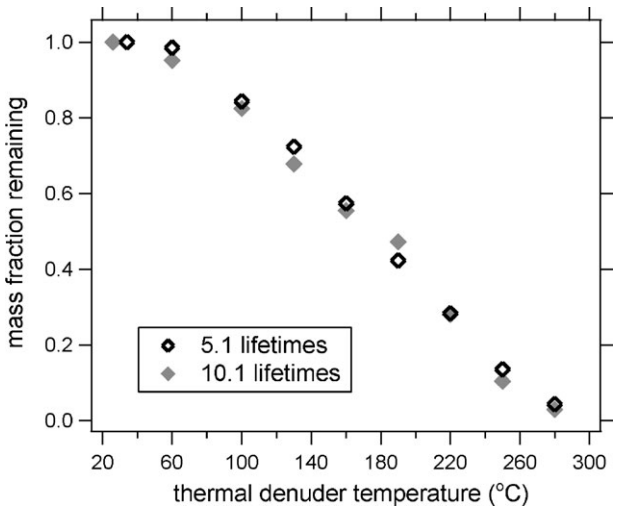

Fig. 6 Volatility measurements of particulate organics after differing amounts of heterogeneous oxidation (corresponding to 5.1 and 10.1 lifetimes), obtained by measuring particle mass downstream of a thermodenuder. The thermograms for the two lifetimes are nearly identical, indicating the volatilities are similar. This suggests the importance of the loss of small, volatile fragments from the particulate organics (Fig. 5, pathway 2) leading to a decrease in particulate carbon but little change in volatility.

(also due to the lack of α-hydrogens), and under our experimental conditions appear not to react with other organics to an appreciable extent,[19] and therefore will mostly dissociate. Thus the formation and fragmentation of alkoxy radicals is likely a major channel for species with several tertiary carbons. Compounds which are substantially less branched, such as *n*-alkanes, may undergo less fragmentation, and thus may have lower fragmentation branching ratios than those measured in the present study. Nonetheless, even for unbranched organics, fragmentation is still expected to be a major channel at high O/C ratios, due to the promotion of alkoxy radical dissociation by oxygen-containing functional groups.

The substantial differences in the chemical composition of organics that have undergone relatively little heterogeneous oxidation (0–3 lifetimes) *versus* those that have undergone substantial oxidation (>5 lifetimes) are illustrated by the evolution of important AMS marker ions. Shown in Fig. 7 are the absolute abundances (mass fraction multiplied by particle mass) of two ions commonly used as markers for oxidized organics, $C_2H_3O^+$ (nominal mass m/z 43) and CO_2^+ (nominal mass m/z 44) as a function of oxidation lifetimes (CO_2^+ is multiplied by 7 to put the two on the same scale). Also shown are the amounts of oxygen added and carbon lost from heterogeneous oxidation (from Table 2; the amount of carbon lost is determined by subtracting the measured carbon content from its maximum value). The increase in $C_2H_3O^+$ begins immediately upon oxidation, and closely tracks the amount of oxygen added (functionalization), whereas the substantial increase in the more heavily oxidized fragment, CO_2^+, occurs only after further oxidation and closely follows the amount of carbon lost (fragmentation). The correlation between individual ions and reaction pathways suggests that the two may be related, with functionalization reactions forming products that yield significant $C_2H_3O^+$ in the mass

spectrometer (such as carbonyls), and fragmentation reactions forming products that yield CO_2^+ (such as acids). This latter observation suggests that organic acids are formed by reactions associated with C–C bond scission. One possible mechanism involves acylperoxy (RC(O)OO) radicals, which are formed from the oxidation of aldehydes or the decomposition of alkoxy radicals adjacent to a carbonyl group,[14] and which will react with HO_2 or RO_2 to form carboxylic acids and/or peroxyacids. Additionally, the observation of the initial formation of species that yield $C_2H_3O^+$ ions may help explain why chamber-generated SOA (generally formed after just a few generations of oxidation) exhibits mass spectra higher in m/z 43 than m/z 44.[42,43]

Atmospheric implications

This work provides evidence that the cleavage of carbon–carbon bonds (fragmentation) is an important pathway in the formation of highly oxidized (high O/C) organics *via* heterogeneous oxidation. The addition of oxygen-containing functional groups to the carbon skeleton (functionalization) dominates the heterogeneous oxidation of reduced organic particles throughout their entire atmospheric lifetimes, with fragmentation reactions being at most a minor channel. However fragmentation is an important pathway for more oxidized organic species, completely dominating oxidation reactions for moderately oxidized (O/C $\approx$ 0.4) species. Fragmentation leads to the formation of small, volatile molecules which escape into the gas phase and decrease the carbon content of the particle. At the same time, oxygen-containing functional groups add to the sites of the C–C bond breaking, so that the oxygen content of the particulate organics does not change (Fig. 5, pathway 2). As a result, the increase in the O/C ratio of the organic aerosol upon oxidation is driven not by the addition of oxygen but rather by the loss of carbon.

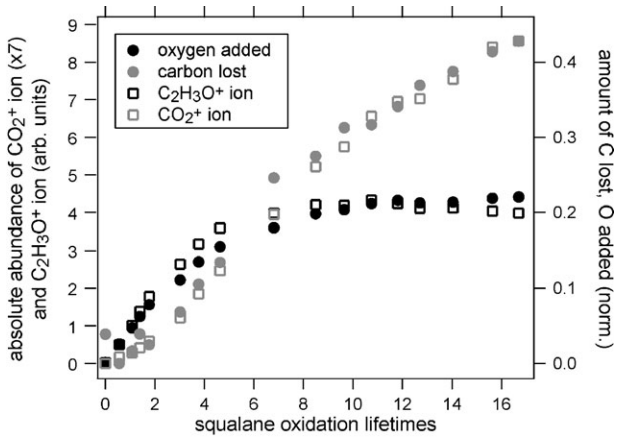

Fig. 7 Absolute abundances of ions used as AMS markers for oxidized organics, CO_2^+ and $C_2H_3O^+$, as a function of extent of oxidation (shown on the same scale by multiplying CO_2^+ by 7). The two ions track the changing abundances of carbon and oxygen (also shown, right axis), suggesting that $C_2H_3O^+$, which increases with initial oxidation, may be a marker for functionalization reactions, while CO_2^+, which increases only with further oxidation, may indicate the importance of fragmentation reactions.

While the experiments carried out in the present study are focused only on the heterogeneous oxidation of particulate organics, it is reasonable to infer that fragmentation may be a key chemical pathway in a wider range of atmospheric oxidation processes, namely the formation of oxygenated organic aerosol (OOA). OOA is highly oxidized (with O/C ratios approaching unity[28]), is ubiquitous in the troposphere[18] and appears to be formed from gas-to-particle conversion (SOA formation) processes.[44,45] Since alkoxy radicals are key intermediates in SOA formation,[15–17] the general conclusions from this work—that oxidized organics fragment upon further oxidation, due to alkoxy radical decomposition—likely apply to the formation of OOA as well (though possible differences are described below). The possible link between fragmentation reactions and OOA formation is supported by the strong correlation between the amount of carbon lost and the abundance of the CO_2^+ ion (a major tracer for OOA) in the aerosol mass spectra (Fig. 7).

These results are consistent with results from several other recent studies which also point to the importance of fragmentation of organics in the formation of highly oxidized organics. In the laboratory generation of OOA from the photooxidation of large (C12 and greater) hydrocarbons, the increase in O/C ratio was found to be much faster,[30,46] and the volatility of the organic aerosol much higher,[46] than what would be expected if the number of carbon atoms per molecule remained constant. In another study involving the photooxidation of wood-burning emissions,[47] the O/C ratio (m/z 44 mass fraction) of the aerosol was found to continually increase even though volatility did not change, which is also seen in the present study (Fig. 6). These laboratory studies all suggest that fragmentation reactions decrease the carbon number of organics during atmospheric oxidation and OOA formation. Additionally, several recent field studies have shown that the photochemical processing increases the O/C ratio of the organic aerosol but not the mass, which necessarily implies a loss of particulate carbon.[45,48,49] This may result from fragmentation reactions of aerosol components, by the gas-phase oxidation of semivolatiles or, if timescales are long enough, by heterogeneous oxidation[48] (though the evaporation of organics, coupled with the condensation of highly oxidized organics from other sources, cannot be ruled out). Taken together, these results suggest that fragmentation reactions may be key steps in the formation of atmospheric OOA, implying that the molecules making up OOA may have fewer carbons than their gas-phase organic precursors.

In this work we have presented measurements of the competition between fragmentation and functionalization channels in atmospheric oxidation (Fig. 4b). To our knowledge this constitutes the first quantitative determination of such branching ratios for organic species spanning a wide range of oxidation; however it should be noted that these results are not necessarily universal for all organics under all atmospheric conditions. Deviations from these measured values may result from several factors. (1) As noted above, structural details of the carbon skeleton have a major influence on alkoxy radical chemistry. Organics that are significantly less branched than squalane, or that have other moieties such as double bonds or rings, may have substantially

different fragmentation–functionalization branching ratios.[14,17] (2) Branching ratios may be sensitive to reaction conditions, such as NO_x level, which affects yields of alkoxy radicals, and aerosol loading, which controls semivolatile partitioning and hence might affect the degree of volatilization. (3) The 254 nm light used to generate OH may photolyze oxidized organics (such as carbonyls), which would lead to more fragmentation than would occur in the ambient atmosphere. (4) Finally, the branching ratios in the gas phase may be different from those in the present heterogeneous oxidation experiments, as reactions that occur in one phase may not be important in the other, such as alkoxy radical isomerization in the gas phase,[14] or reactions between alkoxy radicals and organic molecules in the condensed phase. In order to obtain a quantitative understanding of the competition between fragmentation and functionalization reactions for all atmospheric oxidation processes, these differences need to be explored in future work. Nonetheless, the present study provides evidence that fragmentation of organics is an important chemical pathway in the formation of highly oxidized organics (and particularly OOA) in the atmosphere, and the measured branching ratios provide new experimental constraints for including the effects of photochemical processing in models of organic aerosol formation and evolution.

Acknowledgements

Part of this work was supported by the Director, Office of Energy Research, Office of Basic Energy Sciences, Chemical Sciences Division of the U.S. Department of Energy under Contract No. DE-AC02-05CH11231. J.D.S. is supported by the Camille and Henry Dreyfus foundation postdoctoral program in environmental chemistry. D.L.C. is grateful to the National Aeronautics and Space Administration for support on Grant NASA-NNG06GGF26G.

References

1 A. H. Goldstein and I. E. Galbally, *Environ. Sci. Technol.*, 2007, **41**, 1514.
2 J. R. Odum, T. Hoffmann, F. Bowman, D. Collins, R. C. Flagan and J. H. Seinfeld, *Environ. Sci. Technol.*, 1996, **30**, 2580.
3 N. M. Donahue, A. L. Robinson, C. O. Stanier and S. N. Pandis, *Environ. Sci. Technol.*, 2006, **40**, 2635.
4 Y. J. Balkanski, D. J. Jacob, G. M. Gardner, W. C. Graustein and K. K. Turekian, *J. Geophys. Res., [Atmos.]*, 1993, **98**, 20573.
5 C. L. Heald, D. J. Jacob, R. J. Park, L. M. Russell, B. J. Huebert, J. H. Seinfeld, H. Liao and R. J. Weber, *Geophys. Res. Lett.*, 2005, **32**, L18809.
6 J. A. de Gouw, A. M. Middlebrook, C. Warneke, P. D. Goldan, W. C. Kuster, J. M. Roberts, F. C. Fehsenfeld, D. R. Worsnop, M. R. Canagaratna, A. A. P. Pszenny, W. C. Keene, M. Marchewka, S. B. Bertman and T. S. Bates, *J. Geophys. Res., [Atmos.]*, 2005, **110**, D16305.
7 R. E. Morris, B. Koo, A. Guenther, G. Yarwood, D. McNally, T. W. Tesche, G. Tonnesen, J. Boylan and P. Brewer, *Atmos. Environ.*, 2006, **40**, 4960.
8 A. L. Robinson, N. M. Donahue, M. K. Shrivastava, E. A. Weitkamp, A. M. Sage, A. P. Grieshop, T. E. Lane, J. R. Pierce and S. N. Pandis, *Science*, 2007, **315**, 1259.
9 T. E. Lane, N. M. Donahue and S. N. Pandis, *Atmos. Environ.*, 2008, **42**, 7439.
10 M. K. Shrivastava, T. E. Lane, N. M. Donahue, S. N. Pandis and A. L. Robinson, *J. Geophys. Res., [Atmos.]*, 2008, **113**, D18301.
11 K. C. Barsanti and J. F. Pankow, *Atmos. Environ.*, 2004, **38**, 4371.
12 M. Kalberer, D. Paulsen, M. Sax, M. Steinbacher, J. Dommen, A. S. H. Prévôt, R. Fisseha, E. Weingartner, V. Frankevich, R. Zenobi and U. Baltensperger, *Science*, 2004, **303**, 1659.
13 J. D. Surratt, J. H. Kroll, T. E. Kleindienst, E. O. Edney, M. Claeys, A. Sorooshian, N. L. Ng, J. H. Offenberg, M. Lewandowski, M. Jaoui, R. C. Flagan and J. H. Seinfeld, *Environ. Sci. Technol.*, 2007, **41**, 517.
14 R. Atkinson, *Atmos. Environ.*, 2007, **41**, 8468.
15 H. M. Gong, A. Matsunaga and P. J. Ziemann, *J. Phys. Chem. A*, 2005, **109**, 4312.
16 Y. B. Lim and P. J. Ziemann, *Environ. Sci. Technol.*, 2005, **39**, 9229.
17 Y. B. Lim and P. J. Ziemann, *Environ. Sci. Technol.*, 2009, **43**, 2328.
18 Q. Zhang, J. L. Jimenez, M. R. Canagaratna, J. D. Allan, H. Coe, I. Ulbrich, M. R. Alfarra, A. Takami, A. M. Middlebrook, Y. L. Sun, K. Dzepina, E. Dunlea, K. Docherty, P. F. DeCarlo, D. Salcedo, T. Onasch, J. T. Jayne, T. Miyoshi, A. Shimono, S. Hatakeyama, N. Takegawa, Y. Kondo, J. Schneider, F. Drewnick, S. Borrmann, S. Weimer, K. Demerjian, P. Williams, K. Bower, R. Bahreini, L. Cottrell, R. J. Griffin, J. Rautiainen, J. Y. Sun, Y. M. Zhang and D. R. Worsnop, *Geophys. Res. Lett.*, 2007, **34**, L13801.
19 J. D. Smith, J. H. Kroll, C. D. Cappa, D. L. Che, C. L. Liu, M. Ahmed, S. R. Leone, D. R. Worsnop and K. R. Wilson, *Atmos. Chem. Phys.*, 2009, **9**, 3209–3222.
20 I. L. George, A. Vlasenko, J. G. Slowik, K. Broekhuizen and J. P. D. Abbatt, *Atmos. Chem. Phys.*, 2007, **7**, 4187.
21 J. D. Hearn, L. H. Renbaum, X. Wang and G. D. Smith, *Phys. Chem. Chem. Phys.*, 2007, **9**, 4803.
22 D. L. Che, J. D. Smith, S. R. Leone, M. Ahmed and K. R. Wilson, *Phys. Chem. Chem. Phys.*, 2009, DOI: 10.1039/b904418c.
23 J. T. Jayne, D. C. Leard, X. F. Zhang, P. Davidovits, K. A. Smith, C. E. Kolb and D. R. Worsnop, *Aerosol Sci. Technol.*, 2000, **33**, 49.
24 P. F. DeCarlo, J. R. Kimmel, A. Trimborn, M. J. Northway, J. T. Jayne, A. C. Aiken, M. Gonin, K. Fuhrer, T. Horvath, K. Docherty, D. R. Worsnop and J. L. Jiménez, *Anal. Chem.*, 2006, **78**, 8281.
25 A. P. Grieshop, N. M. Donahue and A. L. Robinson, *Geophys. Res. Lett.*, 2007, **34**, L14810.
26 M. J. Northway, J. T. Jayne, D. W. Toohey, M. R. Canagaratna, A. Trimborn, K. I. Akiyama, A. Shimono, J. L. Jimenez, P. F. DeCarlo, K. R. Wilson and D. R. Worsnop, *Aerosol Sci. Technol.*, 2007, **41**, 828.
27 A. C. Aiken, P. F. DeCarlo and J. L. Jimenez, *Anal. Chem.*, 2007, **79**, 8350.
28 A. C. Aiken, P. F. DeCarlo, J. H. Kroll, D. R. Worsnop, J. A. Huffman, K. Docherty, I. M. Ulbrich, C. Mohr, J. R. Kimmel, D. Sueper, Q. Zhang, Y. Sun, A. Trimborn, M. Northway, P. J. Ziemann, M. R. Canagaratna, R. Alfarra, A. Prevot, J. Dommen, J. Duplissy, A. Metzger, U. Baltensperger and J. L. Jiménez, *Environ. Sci. Technol.*, 2008, **42**, 4478.
29 P. DeCarlo, J. G. Slowik, D. R. Worsnop, P. Davidovits and J. L. Jiménez, *Aerosol Sci. Technol.*, 2004, **38**, 1185–1205.
30 A. L. Robinson, N. M. Donahue and W. F. Rogge, *J. Geophys. Res., [Atmos.]*, 2006, **111**, D03302.
31 J. E. Shilling, Q. Chen, S. M. King, T. Rosenoern, J. H. Kroll, D. R. Worsnop, P. F. DeCarlo, A. C. Aiken, D. Sueper, J. L. Jimenez and S. T. Martin, *Atmos. Chem. Phys.*, 2009, **9**, 771.
32 J. E. Shilling, Q. Chen, S. M. King, T. Rosenoern, J. H. Kroll, D. R. Worsnop, K. A. McKinney and S. T. Martin, *Atmos. Chem. Phys.*, 2008, **8**, 2073.
33 J. F. Pankow and K. C. Barsanti, *Atmos. Environ.*, 2009, **43**, 2829.
34 M. J. Molina, A. V. Ivanov, S. Trakhtenberg and L. T. Molina, *Geophys. Res. Lett.*, 2004, **31**, L22104.
35 A. Vlasenko, I. J. George and J. P. D. Abbatt, *J. Phys. Chem. A*, 2008, **112**, 1552.
36 T. L. Eliason, J. B. Gilman and V. Vaida, *Atmos. Environ.*, 2004, **38**, 1367.
37 K. S. Docherty and P. J. Ziemann, *J. Phys. Chem. A*, 2006, **110**, 3567.
38 D. A. Knopf, J. Mak, S. Gross and A. K. Bertram, *Geophys. Res. Lett.*, 2006, **33**, L17816.

39 V. F. McNeill, R. L. N. Yatavelli, J. A. Thornton, C. B. Stipe and O. Landgrebe, *Atmos. Chem. Phys.*, 2008, **8**, 5465.
40 E. S. C. Kwok and R. Atkinson, *Atmos. Environ.*, 1995, **29**, 1685.
41 G. A. Russell, *J. Am. Chem. Soc.*, 1957, **79**, 3871–3877.
42 R. Bahreini, M. D. Keywood, N. L. Ng, V. Varutbangkul, S. Gao, R. C. Flagan, J. H. Seinfeld, D. R. Worsnop and J. L. Jimenez, *Environ. Sci. Technol.*, 2005, **39**, 5674.
43 M. R. Alfarra, D. Paulsen, M. Gysel, A. A. Garforth, J. Dommen, A. S. H. Prévôt, D. R. Worsnop, U. Baltensperger and H. Coe, *Atmos. Chem. Phys.*, 2006, **6**, 5279.
44 Q. Zhang, D. R. Worsnop, M. R. Canagaratna and J. L. Jimenez, *Atmos. Chem. Phys.*, 2005, **5**, 3289.
45 P. F. DeCarlo, E. J. Dunlea, J. R. Kimmel, A. C. Aiken, D. Sueper, J. Crounse, P. O. Wennberg, L. Emmons, Y. Shinozuka, A. Clarke, J. Zhou, J. Tomlinson, D. R. Collins, D. Knapp, A. J. Weinheimer, D. D. Montzka, T. Campos and J. L. Jimenez, *Atmos. Chem. Phys.*, 2008, **8**, 4027.
46 A. A. Presto, M. A. Miracolo, N. M. Donahue, A. L. Robinson, J. H. Kroll and D. R. Worsnop, *Environ. Sci. Technol.*, 2009, **43**, 4744–4749.
47 A. P. Grieshop, N. M. Donahue and A. L. Robinson, *Atmos. Chem. Phys.*, 2009, **9**, 2227–2240.
48 E. J. Dunlea, P. F. DeCarlo, A. C. Aiken, J. R. Kimmel, R. E. Peltier, R. J. Weber, J. Tomlinson, D. R. Collins, Y. Shinozuka, C. S. McNaughton, S. G. Howell, A. D. Clarke, L. K. Emmons, E. C. Apel, G. G. Pfister, A. van Donkelaar, R. V. Martin, D. B. Millet, C. L. Heald and J. L. Jimenez, *Atmos. Chem. Phys. Discuss.*, 2008, **8**, 15375.
49 G. Capes, B. Johnson, G. McFiggans, P. I. Williams, J. Haywood and H. Coe, *J. Geophys. Res., [Atmos.]*, 2008, **113**, D00C15.

